A Logic Framework for Multiphase Multichannel Image Segmentation

Keegan,M. Sandberg,B. Chan,T.

May 26, 2010

1 Introduction

Variational segmentation (or object detection) algorithms in images are usually framed in the following way: find the function u, within an appropriate function space, that minimizes an energy functional $E(u)$ of the form

$$E(u) = J(u) + \lambda F(u).$$

The energy functional is the weighted sum of a data fidelity term $F(u)$ that penalizes functions that do not adhere to information from the image sufficiently, and a term $J(u)$ that ensures that a minimizer satisfies some regularity assumptions. Regularity is necessary so that anomalies in the image acquisition and communication, such as noise, cannot overly influence the segmentation result. The parameter λ balances the relative importance between data fidelity and regularity. The precise class of such models that we will consider are reviewed in section 2.

Most segmentation models propose novel approaches to either the regularization or the fidelity to the image (or to some reformulation if the energy in (1)), but generally consider the case of a single image. In this paper, we consider the case where vector-valued images of a scene are available. The need for vector-valued images is widespread in image processing applications, such as color images (for example, using RGB or luminance color spaces), medical imagery (separate CT, PET or MRI modalities), satellite imagery (such as hyper-spectral), video sequences, stereo segmentation and various texture modalities. A segmentation is thus conducted using the information from all the components of the vector.

We mention some work that has been done in vector image processing. The Color Snakes model of Sapiro[15] segments a vector-valued image by using a model that in essence detects vector-valued edges. Some image restoration models extend to vector-valued images, such as anisotropic diffusion models[16, 17] and vector-valued total variation models[1]. Region-based scalar segmentation models also extend to vector-valued segmentation[3, 21].

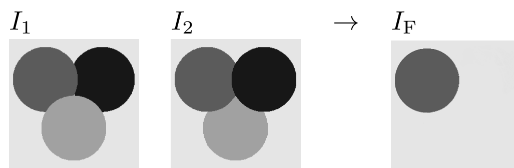

Figure 1

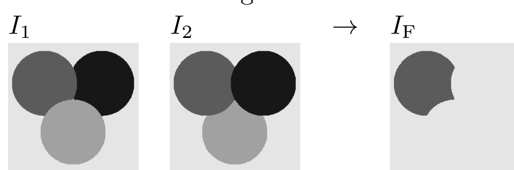

Figure 2

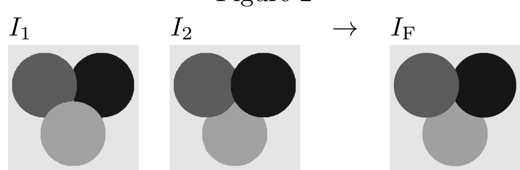

Figure 3

All of the image-based variational models mentioned above offer algorithms that converge to a single solution (modulo setting parameters and initializations). This restriction to a single solution does not address the possibility that information from different sources (such as separate images) can be combined in multiple ways. For example, consider the two images on the left in Figure 1. If the upper-left circle is the object of interest, most algorithms would be unable to obtain the entire circle in a single segmentation although it is clear that every point of the circle is visible in at least one of the available images. If the goal of our segmentation was to segment the entire circle, the result we would get would be the image on the right of Figure 1.

To show an example of this consider Figures 4 and 5.

In Figure 4, there are two images each with 3 separate regions seen in different states of occlusion. In Figure 5 six possible ways of combining the region data from the two channels are shown, any of which may be correct depending on the application. Most multi-channel methods would fail to differentiate between these, and in fact may fail to find any of them. For a demonstration of this, see the example in Figure 7 which we will discuss later.

Any of the images given in Figure 5 can be considered as the correct solution. This depends on the context of the application or interpretation of the segmentation with or without *a priori* information. We offer a framework by which any of the solutions given in Figure 5 can be found, depending on application needs. These images were computed using our method, which we shall discuss

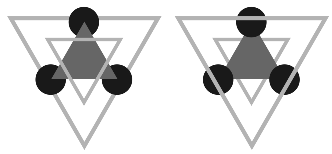

Figure 4: Two images each containing three regions in various states of occlusion.

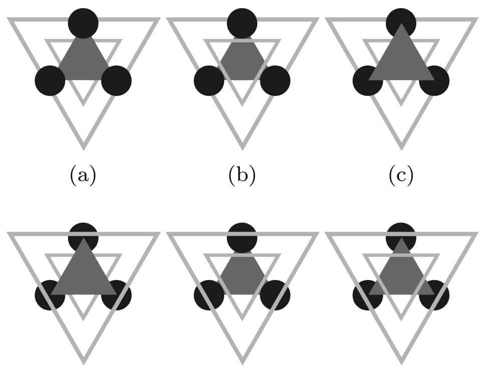

(a) (b) (c)

(d) (e) (f)

Figure 5: The six results obtained from the two images shown in Figure 4 according to the six different ways of combining the channels during segmentation.

inlater sections.

This paper has two parts. Firstly, we propose a general framework by which a segmentation method can be devised. The framework describes how to model the combination of information from the separate sources using a simple set-theory based description. Each of the possible solutions given in Figure 5 can be described by the set operations of union, intersection and compliment on the separate regions in each channel. An intuitive example of this is shown in Figure 6 where it is demonstrated how the set operations are used to combine corresponding regions from separate images to obtained the segmentation in Figure 5a. Our framework allows the user to choose which of these sets of logical operations are appropriate for a given application.

Secondly, we offer a specific algorithm that may be used for solving such a segmentation. The numerical algorithm uses level-set methods to solve the Active Contours Without Edges (ACWE) variational model, which has been extensively studied in a group of papers. The original model [4] found a binary segmentation of an image, and subsequent efforts extended this to multiple region segmentations [3] (multiphase or multi-label) and segmentations of vector-valued images [19] (multichannel). In particular, we continue the work introduced by the Logic Framework of [14] in which was introduced the combination of information from different channels in terms of logic and set theory. The

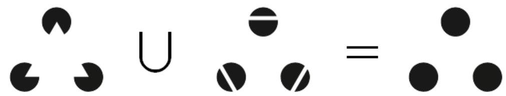

(a) Channel Combination of Region 1

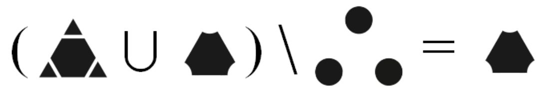

(b) Channel Combination of Region 2

(c) Channel Combination of Region 3

Figure 6: The above three images give an intuitive demonstration of how the corresponding regions in each image of Figure 4 are combined using the language of set theory to obtain the segmentation shown in Figure 5a

Logic Framework, however, was only defined for binary segmentations. Here we extend this idea to multiphase problems.

2 Background on a Variational model

Consider the domain $\Omega \subset \mathbb{R}^2$ that is made up of m regions. The goal of multiphase segmentation is to make a determination of the exact position of the m regions. We denote our guesses of the m regions as the disjoint sets $R^1, ..., R^m$, where $\cup_{j=1}^m R^j = \Omega$. In the case where we have only one image, $I(x) : \Omega \to [0,1]$, we determine the regions by assuming some region classification scheme that we can match the regions to. The Active Contours Without Edges (ACWE) model makes the assumption that the image can be approximated by a piecewise constant function. The multiphase version of the method is formulated as: find the values $c_1, ..., c_m$ and the curve $C = \cup_{j=1}^m \partial R^j$ that minimizes the energy functional

$$\text{length}(C) + \lambda \sum_{j=1}^{m} \int_{R^j} (I(x) - c^j)^2 . \, dx$$

To extend this to multiple images (the multichannel problem), the segmentation algorithm must combine data from all channels to classify the regions. There are two approaches to take in this. Firstly, each image can be segmented separately and then combined to form a unique segmentation. Secondly, you can incorporate informaton from all images together in a single segmentation procedure. In [15, 14] it has been argued that the first approach has drawbacks.

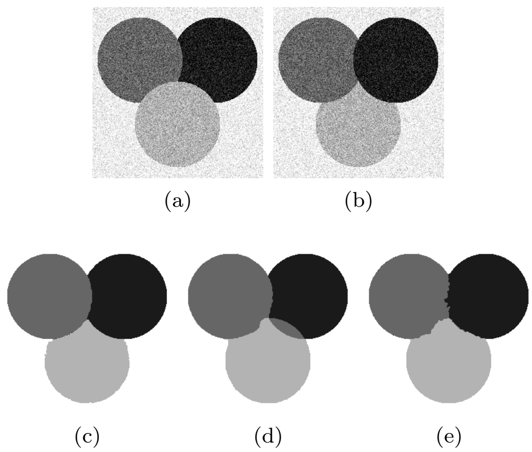

(a) (b)

(c) (d) (e)

Figure 7: A demonstration of different multichannel multiphase segmentation methods for the images in (a) and (b). In (c) is shown the results from our method. In (d) is shown the results of minimizing the energy in (2) without scaling of the data variable (see Section 3.2). This is caused by the fact that in a multiphase application, a simple summing of the energies does not behave well in regions of conflict between the channels. In (e) is shown the results of minimizing the energy in (2) with scaling. Here we see the objective conflict of the data fidelity terms in the regions of conflict between the channels.

For instance, it is more expensive and results are less robust to noise. Thus we take the second approach.

The most common way to extend a single channel algorithm to a many channel algorithm is to sum the contributions from each channel, such as for the 2-phase ACWE model [19]. We can do this for the multiphase case in an identical manner. If we have n images, denoted $I_k(x) : \Omega \to [0, 1]$ for $k = 1, ..., n$, we can define a multiphase multichannel ACWE model as: determine the constant values c_k^j, $j = 1, ..., m$ and $k = 1, ..., n$ of region j in channel k and the curve $C = \cup_{j=1}^m \partial R^j$ that minimizes

$$\text{length}(C) + \lambda \sum_{j=1}^{m} \int_{R^j} \frac{1}{n} \sum_{k=1}^{n} (I_k(x) - c_k^j)^2 \, dx$$

This corresponds to simply averaging the contributions from each channel. Problems occur when channels give conflicting information, since it is unclear how to settle the conflict. It has been shown in the 2-phase case [14] that such conflicts can cause local minima in the energy functional and and that the results of an algorithm can depend heavily on the initial labeling of the regions. An example of the drawbacks of using the energy in (2) in the multiphase case are shown in Figure 7.

In the 2-phase case, the Logic Framework [14] was proposed to avoid this conflict by altering the way in which the data fidelity terms from each channel are combined. To simplify and generalize this discussion, we define some further notation. Let the data variables

$$\begin{array}{ll} z_k^{\text{in}}(x) & = \left(I_k(x) - c_k^{\text{in}}\right)^2 \\ z_k^{\text{out}}(x) & = \left(I_k(x) - c_k^{\text{out}}\right)^2 \end{array} \tag{1}$$

be the data fitting functions for each channel k and the two regions (corresponding to inside and outside the curve C, R^{in} and R^{out}). Furthermore we define the combination operators for each region $f^{\text{in}}(x)$ and $f^{\text{out}}(x)$, which implicitly contain the data fidelity from each channel

$$f^j(x) = f^j(z_1^j(x), ..., z_n^j(x)). \tag{2}$$

Thus the 2-phase generalized ACWE energy can be written as

$$\text{length}(C) + \lambda \int_{R^{\text{in}}} f^{\text{in}}(x)\, dx + \lambda \int_{R^{\text{out}}} f^{\text{out}}(x)\, dx.$$

In the simplest case, the combination operators $f^{\text{in}}(x)$ and $f^{\text{out}}(x)$ are chosen as some permutation of the operators $f_\cup(x)$ and $f_\cap(x)$ where

$$\begin{array}{ll} f_\cap(x) & = 1 - \left\{\prod_{k=1}^n \left(1 - z_k^j(x)\right)\right\}^{\frac{1}{n}}, \\ f_\cup(x) & = \left\{\prod_{k=1}^n z_k^j(x)\right\}^{\frac{1}{n}}. \end{array} \tag{3}$$

In more complicated cases, the combination operators can be compositions of $f_\cup(x)$ and $f_\cap(x)$ in lower dimensions and the operator

$$f_c(z_k^j(x)) = 1 - z_k^j(x). \tag{4}$$

The operators in (3) and (4) correspond to the intersection, union and compliment rules for combining data from each channel, which can be seen in particular in the case where the data variables are binary. In the simple case, the choice of the $f_\cup(x)$ and $f_\cap(x)$ prevents conflicting objectives between the terms of each region by strictly defining how such conflicts are resolved. Alternative combination operators that serve the same purpose as the Logic operators have since been proposed by Moelich [10] and Israel-Jost et al. [7, 6]. In fact [7] highlights the fact that there is a great deal of literature dedicated to the study of such combination operators and their properties. A discussion and references can be found in the bibliography of that article. Using this information [6, 7] proposes the minimum and maximum operators, which act more decisively on conflictive channels than those in (3),

$$\begin{array}{ll} f_\cap(x) & = \max_{k=1,..,n} z_k^j(x) \\ f_\cup(x) & = \min_{k=1,..,n} z_k^j(x) \end{array} \tag{5}$$

In the next section, we extend the Logic Framework to multiphase problems.

3 The Logic Framework for Multiphase Segmentation

3.1 General Framework

The general form of the multiphase ACWE energy that we propose is written as

$$\text{length}(C) + \lambda \sum_{j=1}^{m} \int_{R^j} f^j(x)\, dx$$

where $f^j(x)$ denotes the combination operator of region j as in (2). To describe how we choose to define the combination operators, we consider the ideal case where the logic variables give region information with complete certainty, namely they are binary functions,

$$z_k^j(x) = \begin{cases} 0 & \text{if } x \in R_k^j, \\ 1 & \text{otherwise.} \end{cases} \tag{6}$$

In this case the operators in both (3) and (5) act precisely as the intersection and union operators. In the multiphase case we again construct our combination operators out of the set operations, however with more than two regions we need to combine and compose the operators in more complicated ways. The constraint we impose on the choice of operators is the following:

> *If the logic variables are binary i.e. of the form (6), then for each $x \in \Omega$, there is exactly one $j = 1, ..., k$ such that $f^j(x) = 0$ and $f^i(x) = 1$ for all $i \neq j$.*

This constraint is fairly unrestrictive, but it prevents conflictive objectives between the region fidelity terms and ensures that all points are labelled to a region.

We impose this constraint in the following way: we order the regions according to some preference. To simplify this exposition, we assume the ordering corresponds to the numerical ordering of the regions. This preference can be interpreted as the order of occlusions in the image, so that the algorithm prioritizes the segmentation of each region by their ordering. Thus each point is labelled to the highest ordered region in which the point can be found in any single image. In terms of the characteristic functions and set operations, the combination operators for each region can described as

$$\begin{array}{rcl} R^1 & = & \cup_{k=1}^n R_k^1 \\ R^2 & = & \cup_{k=1}^n R_k^2 \setminus \cup_{k=1}^n R_k^1 \\ R^3 & = & \cup_{k=1}^n R_k^3 \setminus \left(\cup_{k=1}^n R_k^1 \bigcup \cup_{k=1}^n R_k^2 \right) \\ & \vdots & \\ R^m & = & \cap_{k=1}^n R_k^m \end{array} \tag{7}$$

In terms of the set-operation operators, the combination operators are written as

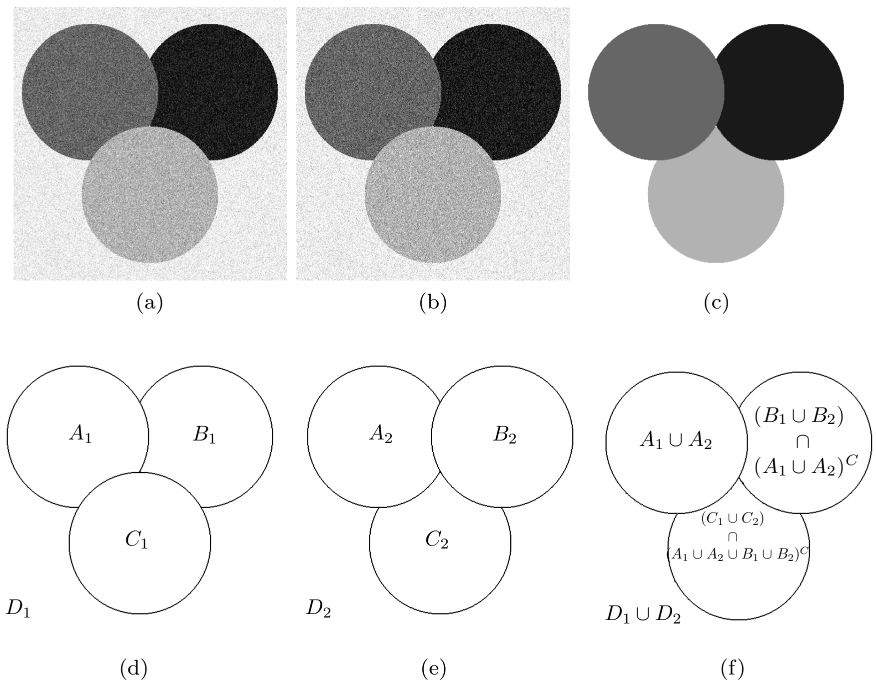

Figure 8: Figure (c) shows the result of a segmentation of the images in (a) and (b). Figure (f) gives a clear demonstration of the set-theory operators used to model the segmentation using the regions for the images shown in (d) and (e).

$$
\begin{array}{lcl}
f^1(z_1^1, ..., z_n^1) & = & f_\cup(z_1^1, ..., z_n^1) \\
f^2(z_1^2, ..., z_n^2) & = & f_\cap(f_\cup(z_1^2, ..., z_n^2), f_c(f_\cup(z_1^1, ..., z_n^1))) \\
f^3(z_1^3, ..., z_n^3) & = & f_\cap\Big[f_\cup(z_1^3, ..., z_n^3), f_c\Big(f_\cup\big(f_\cup(z_1^1, ..., z_n^1), f_\cup(z_1^2, ..., z_n^2)\big)\Big)\Big] \\
 & \vdots & \\
f^m(z_1^m, ..., z_n^m) & = & f_\cap(z_1^m, ..., z_n^m)
\end{array}
\tag{8}
$$

For our own experiments, we adopt the operators of Israel-Jost et al. in (5) and the compliment operator in (4). Figures 4 and 8 give intuitive demonstrations of this use of the combination operators.

3.2 Variable Scaling

Because the differences between intensity averages of regions in the multiphase case are a fraction of the intensity range of the images (namely smaller than 1), the data variables given in equation (1) might not give an accurate measure of the discrepancy in intensity from the average intensity in a given region. Thus we adopt a scaling of the error terms in (1) that can give a better measure of the discrepancy. We choose an exponential scaling as first proposed in [10], which the author aptly named the exponential logic model,

$$z_k^j(x) = \exp\{-\gamma(I_k(x) - c_k^j)\} \tag{9}$$

The parameter γ is chosen based on the expected differences in mean between the regions.

4 Level Set Formulation

Level set methods [11, 12, 20] have been widely used in image segmentation problems including in the original ACWE model, see [9, 2, 4, 18]. For the level-set based multiphase segmentation methods their have been a number of approaches proposed to model the regions: N level-set functions for N regions [13, 20], N level-set functions for 2^N regions [19] and a single level-set function for N regions (a multilayer function)[5, 8].

Recently there have been many algorithms proposed that solve for the multi-label segmentation problem. In fact many of these have proposed alternative level set algorithms or level set-like methods. However, for ease of explanation we will describe a level set based implementation based on the method described in [19], and leave the implementation using other approaches to future work or the interested reader.

For simplicity we will describe the 4-phase case, for which two level sets are required. We denote the two level sets by ϕ_1 and ϕ_2. The curves described by the sets $\{\phi_1 = 0\}$ and $\{\phi_2 = 0\}$ indicate boundaries between the regions, while the regions themselves are identified by some combination of the sets $\{\phi_1 > 0\}$, $\{\phi_1 < 0\}$, $\{\phi_2 > 0\}$ and $\{\phi_2 < 0\}$. The regions are chosen by the following combinations: region 1 is the intersection of the regions $\{\phi_1 > 0\}$ and $\{\phi_2 > 0\}$, region 2 by the intersection of $\{\phi_1 < 0\}$ and $\{\phi_2 > 0\}$, region 3 by the intersection of $\{\phi_1 > 0\}$ and $\{\phi_2 < 0\}$, and region 4 by the intersection of $\{\phi_1 < 0\}$ and $\{\phi_2 < 0\}$. In the general case, n level sets allow you to describe upto 2^n regions.

To describe the regions we use the functions δ_ϵ and H_ϵ, defined as

$$\begin{aligned}
\delta_\epsilon(\phi(x)) &= \frac{\epsilon}{\pi(\epsilon^2 + \phi(x)^2)} \\
H_\epsilon(\phi(x)) &= \frac{1}{2}\left(1 + \frac{2}{\pi}\arctan\left(\frac{\phi(x)}{\epsilon}\right)\right),
\end{aligned}$$

numerically approximate the delta and Heaviside functions,

$$\begin{aligned}
\delta_0(\phi(x)) &= \frac{d}{d\phi(x)} H_0(\phi(x)) \\
H_0(\phi(x)) &= \begin{cases} 1 & \text{for } \phi(x) \geq 0, \\ 0 & \text{otherwise.} \end{cases}
\end{aligned}$$

Using the max/min operators (5) for the channel combination, the combination operators for the four channels are

$$
\begin{aligned}
f^1(x) &= \min\{z_1^1(x), ..., z_n^1(x)\} \\
f^2(x) &= \max\left[\min\{z_1^2(x), ..., z_n^2(x)\}, 1 - \min\{z_1^1(x), ..., z_n^1(x)\}\right] \\
f^3(x) &= \max\left[\min\{z_1^3(x), ..., z_n^3(x)\}, ... \right. \\
&\qquad \left. 1 - \min\left\{\min\{z_1^1(x), ..., z_n^1(x)\}, \min\{z_1^2(x), ..., z_n^2(x)\}\right\}\right] \\
f^4(x) &= \max\{z_1^4(x), ..., z_n^4(x)\}
\end{aligned}
$$

where we adopt the data variables $z_j^k(x)$ are defined as in (9).

Using the level set formulation, the 2-level set ACWE energy can be written as

$$
\begin{aligned}
E(\phi_1, \phi_2) = &\left(\int_\Omega |\nabla H_\epsilon(\phi_1(x))|\, dx + \int_\Omega |\nabla H_\epsilon(\phi_2(x))|\, dx\right) \\
&+ \lambda\bigg(\int_\Omega H_\epsilon(\phi_1(x)) H_\epsilon(\phi_2(x)) f^1(x)\, dx \\
&+ \int_\Omega (1 - H_\epsilon(\phi_1(x))) H_\epsilon(\phi_2(x)) f^2(x)\, dx \\
&+ \int_\Omega H_\epsilon(\phi_1(x))(1 - H_\epsilon(\phi_2(x))) f^3(x)\, dx \\
&+ \int_\Omega (1 - H_\epsilon(\phi_1(x)))(1 - H_\epsilon(\phi_2(x))) f^4(x)\, dx\bigg)
\end{aligned}
\tag{10}
$$

The constant parameter λ controls the weighting between the regularizing term and the data fidelity term. This is minimized by solving for the Euler-Lagrange equations of the energy using artificial time-stepping, written as

$$
\begin{aligned}
\frac{\partial \phi_1(x)}{\partial t} = -\delta_\epsilon(\phi_1(x))\bigg[&-\operatorname{div}\left(\frac{\nabla\phi_1(x)}{|\nabla\phi_1(x)|}\right) + \lambda(f^1(x) - f^2(x)) H_\epsilon(\phi_2(x)) \\
&+ \lambda(f^3(x) - f^4(x))(1 - H_\epsilon(\phi_2(x)))\bigg] \\
\frac{\partial \phi_2(x)}{\partial t} = -\delta_\epsilon(\phi_2(x))\bigg[&-\operatorname{div}\left(\frac{\nabla\phi_2(x)}{|\nabla\phi_2(x)|}\right) + \lambda(f^1(x) - f^3(x)) H_\epsilon(\phi_1(x)) \\
&+ \lambda(f^2(x) - f^4(x))(1 - H_\epsilon(\phi_1(x)))\bigg]
\end{aligned}
$$

For the details of the numerical approximations needed to implement this method see [19, 3] and for more on the numerical implementations of level set methods see [12].

5 Numerical Results

In this section, we show some examples of our method on sets of real world images.

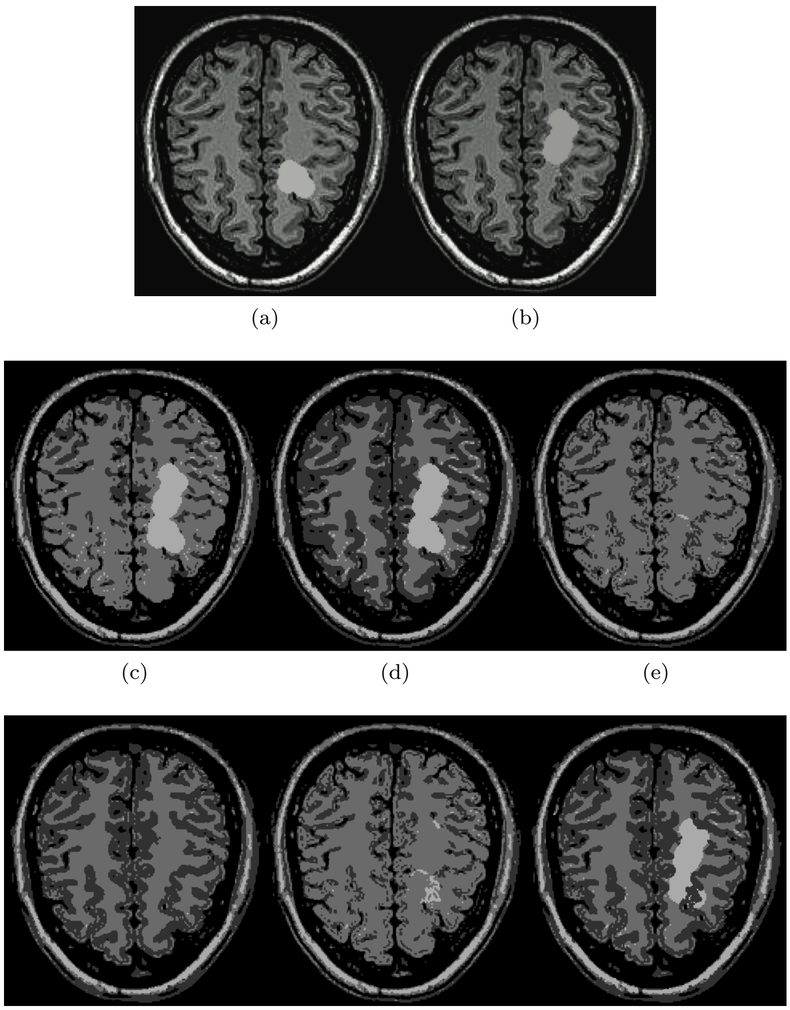

(a) (b)

(c) (d) (e)

(f) (g) (h)

Figure 9

In Figure 9, we show an example of segmenting regions of the brain. In Figures 9a and 9b are shown two brain images with artificial tumors inserted in disjoint positions. We consider this as a 4-region segmentation with three regions consisting of regions of the brain - the grey matter, the white matter and the tumor and bone respectively. The fourth region consists of the black background. Due to the little importance of the background, we essentially treat the problem as a 3-phase problem with the background ordered last in all our results. This gives us six possible solutions that our method computes, according to the possible orderings of the first three regions. These are shown in Figures 9c-h.

In the first two solutions, the region of the tumor is ordered first among the regions. The white matter is ordered second in the (c) and third in (d), and the grey matter is ordered third in (c) and second in (d). In (g) and (h) the tumor region is ordered third, while the white matter and grey matter switch ordering between first and second. Finally, in (e) and (f) the tumor region is ordered second, while the white matter and grey matter switch ordering between first and third.

All the images (c)-(h) provide valuable information about the corresponding regions in each of the two channels. For instance (c) and (d) allow the user to group the tumor regions together, to see the tumor as a whole and also see obtain information about the white matter and gray matter regions. In (c) the white matter is emphasized, and in (d) the grey matter is emphasized. In (g) and (h) the user can ignore the parts of the tumor region that are not in both channels, thus reacquiring all lost information of the white and grey matter regions lost by the presence of the tumor.

References

[1] P. Blomgren and T. F. Chan. Color TV: Total Variation Methods for Restoration for Vector-Valued Images. *IEEE Transactions on Image Processing*, 7(3):304–309, 1998.

[2] V. Caselles, R. Kimmel, and G. Sapiro. Geodesic active contours. *International journal of computer vision*, 22(1):61–79, 1997.

[3] T.F. Chan, B.Y. Sandberg, and L.A. Vese. Active contours without edges for vector-valued images. *Journal of Visual Communication and Image Representation*, 11(2):130–141, 2000.

[4] T.F. Chan and L.A. Vese. Active contours without edges. *IEEE Transactions on Image Processing*, 10(2):266–277, 2001.

[5] G. Chung and L.A. Vese. Image segmentation using a multilayer level-set approach. *Computing and Visulatization in Science*, 12(6):267–285, August 2009.

[6] V. Israel-Jost, E. Breton, E. Angelini, P. Choquet, and I. Bloch. Vectorial multi-phase mouse brain tumor segmentation in T1-T2 MRI. In *IEEE International Symposium on Biomedical Imaging*, 5-8, May 2008.

[7] V. Israel-Jost, J. Darbon, E.D. Angelini, and I. Bloch. Multi-phase and multi-channel region segmentation and application in brain mri. Technical report, UCLA CAM Report 08-75, 2008.

[8] J. Lie, M. Lysaker, and X-C. Tai. A variant of the level set method and applications to image segmentation. *Mathematics of Computation*, 75(255):1155–1174, July 2006.

[9] R. Malladi, J.A. Sethian, and B.C. Vemuri. Shape Modelling with Front Propagation. *IEEE Transactions on Pattern Analysis and Machine Intelligence*, 17:158–175, 1995.

[10] M. Moelich. *Logic Models for Segmentation and Tracking*. PhD thesis, University of California Los Angeles, 2004.

[11] Stanley Osher and James A. Sethian. Fronts propagating with curvature dependent speed: Algorithms based on hamilton-jacobi formulations. *Journal of Computational Physics*, 79(1):12–49, 1988.

[12] Stanley J. Osher and Ronald P. Fedkiw. *Level set methods and dynamic implicit surfaces*. Springer, 1 edition, October 2002.

[13] C. Samson, L. Blanc-Féraud, G. Aubert, and J. Zerubia. A level set model for image classification. *IJCV*, 40(3):187–197, December 2000.

[14] B. Sandberg and T.F. Chan. A logic framework for active contours on multi-channel images. *Journal of Visual Communication and Image Representation*, 16(3):333–358, 2005.

[15] G. Sapiro. Color snakes. *Computer Vision Image Understanding*, 68(2):247–253, 1997.

[16] G. Sapiro and D. L. Ringach. Anisotropic diffusion of multivalued images with applications to color filtering. *Image Processing, IEEE Transactions on*, 5(11):1582–1586, 1996.

[17] J. Shah. Curve evolution and segmentation functionals: application to color images. In *In Proceedings IEEE ICIP'96*, pages 461–464, 1996.

[18] A. Tsai, A. Yezzi, and A. S. Willsky. Curve evolution implementation of the mumford-shah functional for image segmentation, denoising, interpolation, and magnification. *IEEE Transactions on Image Processing*, 10:1169–1186, 2001.

[19] L.A. Vese and T.F. Chan. A multiphase level set framework for image segmentation using the mumford and shah model. *International Journal of Computer Vision*, 50(3):271–293, December 2002.

[20] H.K. Zhao, T. Chan, B. Merriman, and S. Osher. A variational level set approach to multiphase motion. *Journal of Computational Physics*, 1(127):179195, 1995.

[21] S.C. Zhu and A. Yuille. Region competition: unifying snakes, region growing, and bayesian/MDL for multiband image segmentation. *IEEE Tranactions on Pattern Analysis and Machine Intelligence*, 18(9):884–900, 1996.